Cellular Intrinsic Factors Involved in the Resistance of Squamous Cell Carcinoma to Photodynamic Therapy

Yolanda Gilaberte[1], Laura Milla[2], Nerea Salazar[3], Jesús Vera-Alvarez[4], Omar Kourani[3], Alejandra Damian[3], Viviana Rivarola[2], Maria José Roca[4], Jesús Espada[3], Salvador González[5,6] and Angeles Juarranz[3,6]

Photodynamic therapy (PDT) is widely used to treat non-melanoma skin cancer. However, some patients affected with squamous cell carcinoma (SCC) did not respond adequately to PDT with methyl-δ-aminolevulinic acid (MAL-PDT) and the tumors acquired an infiltrative phenotype and became histologically more aggressive, less differentiated, and more fibroblastic. To search for potential factors implicated in SCC resistance to PDT, we have used the SCC-13 cell line (parental) and resistant SCC-13 cells obtained by repeated MAL-PDT treatments (5th and 10th PDT-resistant generations). Xenografts assays in immunodeficient mice showed that the tumors generated by resistant cells were bigger than those induced by parental cells. Comparative genomic hybridization array (aCGH) showed that the three cell types presented amplicons in 3p12.1 *CADM2*, 7p11.2 *EFGR*, and 11q13.3 *CCND1* genes. The 5th and 10th PDT-resistant cells showed an amplicon in 5q11.2 MAP3K1, which was not present in parental cells. The changes detected by aCGH on CCND1, EFGR, and MAP3K1 were confirmed in extracts of SCC-13 cells by reverse-transcriptase PCR and by Western blot, and by immunohistochemistry in human biopsies from persistent tumors after MAL-PDT. Our data suggest that genomic imbalances related to CCND1, EFGR, and particularly MAP3K1 seem to be involved in the development of the resistance of SCC to PDT.

Journal of Investigative Dermatology accepted article preview 9 April 2014; doi:10.1038/jid.2014.178

INTRODUCTION

Non-melanoma skin cancer (NMSC) is the most common malignancy occurring in the White population (Neville *et al.*, 2007; Lomas *et al.*, 2012). NMSC basically comprises basal cell carcinoma and squamous cell carcinoma (SCC). Photodynamic therapy (PDT) has been revealed as an excellent treatment for NMSC. PDT consists in the administration of a photosensitizer, which accumulates preferentially in the tumor, followed by its activation with light. Activation of the photosensitizer induces reactive oxygen species, mainly singlet oxygen ($^1O_2$), that cause cell death and consequently the regression of the tumor (Juarranz *et al.*, 2008; Agostinis *et al.*, 2011). Methyl-δ-aminolevulinic acid–PDT (MAL-PDT), a precursor of the photoactive compound protoporphyrin IX (PpIX) intermediary in the synthesis of heme, is an efficient treatment for NMSC, with resolution rates ranging from 70 to 90% and superior cosmetic outcomes compared with other treatment modalities (Fai *et al.*, 2009; Ortiz-Policarpio and Lui, 2009; Stebbins and Hanke, 2011). According to current guidelines, topical PDT is effective for SCC, but, in view of its metastatic potential, topical PDT cannot currently be recommended for the treatment of invasive SCC (strength of recommendation D, quality of evidence ii–iii) (Morton *et al.*, 2008). Nevertheless, there are some reports of the successful use of MAL-PDT in this tumor in patients who reject any other treatment either for medical or personal reasons (Calzavara-Pinton *et al.*, 2008). We have used MAL-PDT in exceptional patients diagnosed with invasive SCC and had success in some of them, whereas in others the tumor continued to progress. In addition, our group has previously reported that MAL-PDT causes the selection of resistant cells of a SCC cell line (SCC-13) (Rheinwald and Beckett, 1981) after several treatment sessions. PDT-resistant cells showed few differences on intracellular content of the photosensitizer (PpIX) related to the parental cells, but they presented a more fibroblastic morphology, higher capacity to close wounds, more expression of cell–substrate adhesion proteins, and higher expression of p-survivin (Milla *et al.*, 2011).

On the basis of these clinical and experimental observations, we have investigated the genomic alterations that might be implicated in the resistance of SCC to MAL-PDT in patients.

[1]*Unidad de Dermatología, Hospital de San Jorge de Huesca, and Institute of Health Science of Aragón, Zaragoza, Spain;* [2]*Departamento de Biología Molecular, Facultad de Ciencias Exactas, Físico-Químicas y Naturales, Universidad Nacional de Río Cuarto, Córdoba, Argentina;* [3]*Departamento de Biología, Facultad de Ciencias, Universidad Autónoma de Madrid, Madrid, Spain;* [4]*Departamento de Patología, Hospital de San Jorge de Huesca, Huesca, Spain and* [5]*Dermatology Service, Memorial Sloan-Kettering Cancer Center, New York, New York, USA*

[6]*These authors contributed equally to this work.*

Correspondence: Angeles Juarranz, Departamento de Biología, Facultad de Ciencias, Universidad Autónoma de Madrid, Madrid 28049, Spain. E-mail: angeles.juarranz@uam.es

Abbreviations: ALA, δ-aminolevulinic acid; aCGH, Comparative genomic hybridization array; MAL, methyl δ-aminolevulinic acid; NMSC, non-melanoma skin cancer; PDT, photodynamic therapy; SCC, squamous cell carcinoma

Received 30 October 2013; revised 3 March 2014; accepted 14 March 2014

Table 1. Clinical, histological, and immunohistochemical characteristics of SCC of the patients included in the study before MAL-PDT and several months after the treatment

Case	Age	Gender	Location	Histological diagnosis	MAL-PDT	Immunohistochemistry						
						CD31	E-cadherin	KI67	P53	EGFR	Cyclin D1	p-ERK[1]
Patients without response to MAL-PDT												
1	88	Female	Forehead	Moderately differentiated SCC	Before	NI	Positive	+20%	95%	Intense	Positive	Grade 2
			Forehead (recurrence)	Poorly differentiated SCC	After 1 month	NI	Positive	+30%	97%	Intense	Positive	Grade 3
			Parotid gland	SCC metastasis	After 4 months			+20%	80%	Intense	Positive	Negative
2	82	Female	Forehead	Well-differenciated SCC	Before	NI	Positive	+8%	0%	Mild	MIld	Negative
			Forehead (recurrence)	Moderately differentiated infiltrating SCC	After 4 months	NI	Positive	+5%	0%	Moderate	Positive	Grade 3
			Forehead (subcutaneous)	Moderately differentiated infiltrating SCC (subcutaneous recurrence)	After 18 months			+3%	0%	Moderate	Positive	Grade 4
3	89	Male	Scalp	Poorly differentiated SCC	Before	NI	Positive	+100%	1%	Negative	Mild[2]	Grade 1
			Scalp (recurrence)	Poorly differentiated SCC	After 1 month	NI	Positive	+100%	0%	Mild	Mild[2]	Grade 2
Patients with good response to MAL-PDT												
4	91	Female	Forehead	Poorly differentiated SCC with intense inflammatory lymphocytic infiltrate	Before	NI	Positive	+100%	0%	Mild	Negative[3]	Grade 2
5	92	Female	Cheek	Poorly differentiated SCC with intense inflammatory lymphocytic infiltrate	Before	NI	Positive	+25%	0%	Negative	Negative	Negative
6	87	Male	Preauricular	Moderately differentiated SCC with intense inflammatory lymphocitic infiltrate	Before	NI	Positive	+35%	+100%	Negative	Negative[3]	Grade 1

Abbreviations: MAL-PDT, methyl-δ-aminolevulinic acid-photodynamic therapy; NI, no vascular invasion; SCC, squamous cell carcinoma.

[1]the expression of p-ERK was evaluated according to Zhang *et al.* (2007) (grade 1: <5%; grade 2: 5–25%; grade 3: 26–50%; grade 4 >50%). E-cadherin and CD31 were only evaluated in primary SCC, neither in metastasis nor in subcutaneous recurrence.

[2]The intensity of the stain was the same but the percentage of positive cells increased from 4 to 10% after PDT.

[3]Isolated cells were positive but not in significant number.

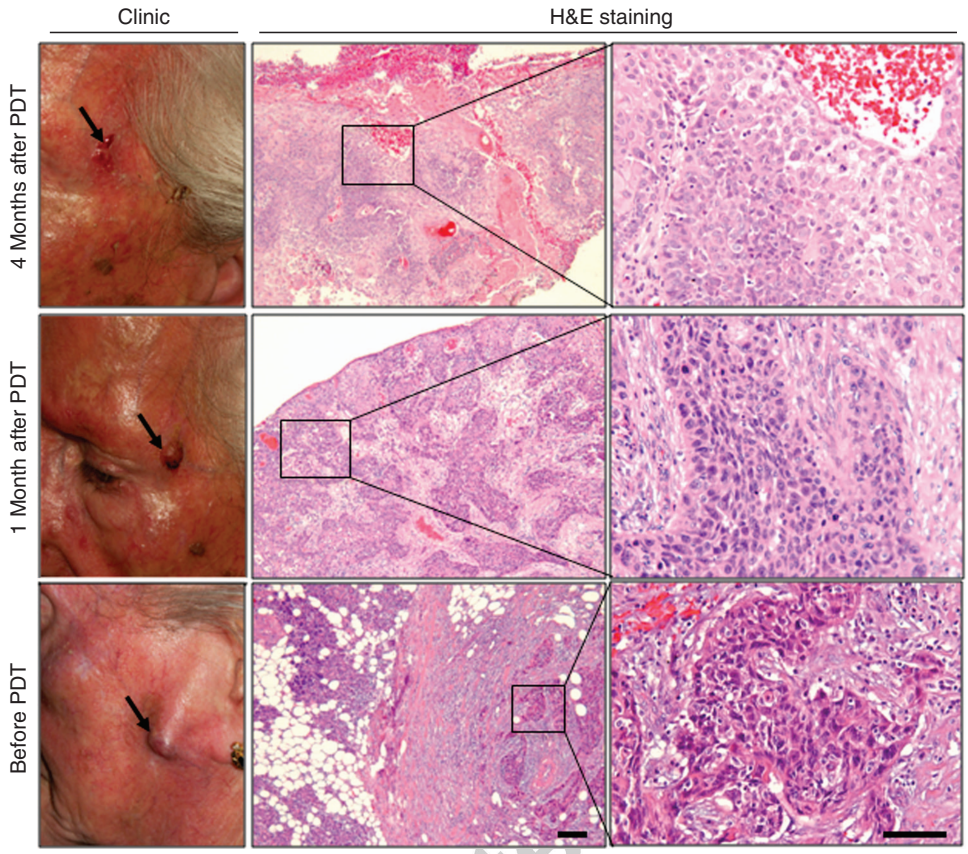

Figure 1. Clinical and histological evolution of a squamous cell carcinoma (SCC) treated with methyl-δ-aminolevulinic acid-photodynamic therapy (PDT). The SCC was located on the left temple of an 88-year-old woman (case 1). Upper panels: clinical SCC at diagnosis (left); the histology shows a moderately differenciated SCC at low and higher magnification (~~medium~~, and right panels, respectively). One month after PDT, the lesion became a poorly differentiated SCC (~~medium~~ panel). Four months later, an indurated tumor appeared on her left preauricular area; the histological diagnosis was parotid gland infiltrated with a poorly differentiated squamous cell carcinoma (lower panels). Notice infiltrating tumoral nests in the stroma of the parotid gland. Arrows indicate the amplified areas showed in the panels on the right. Scale bar = 200 μm. H&E, hematoxylin and eosin.

For that purpose, we have related the lack of response to MAL-PDT in patients affected with cutaneous SCC and the increase of the tumor aggressiveness with alterations in the chromosomal pattern of SCC-13 PDT-resistant cells, determined by comparative genomic hybridization arrays (aCGH).

RESULTS

Patients with SCC treated with MAL-PDT

We have studied six patients diagnosed with invasive cutaneous SCC and treated with two sessions of MAL-PDT (cases 1–6, Table 1). In three of them (cases 1–3) the tumor persisted, recurred, or even metastasized after MAL-PDT (Figure 1; Supplementary Figure S1 online), whereas in the other three patients (cases 4–6) the tumor was cured without recurrence after a follow-up of 24 months. The most striking case was number 1 because the patient died 5 months after developing regional lymphatic metastasis and tumoral infiltration of the parotid gland 4 months after MAL-PDT of SCC on the forehead (Figure 1). Except for case 3, diagnosed from the beginning with poorly differentiated SCC, cases 1 and 2 became histologically less differentiated after MAL-PDT. From a clinical point of view, there were no obvious differences between patients with good or bad response to MAL-PDT, whereas, at the histological level, the most remarkable difference between both situations was the presence of a significant inflammatory lymphocytic infiltrate in the tumors with good response to MAL-PDT, which was absent in those without response (Supplementary Figure S2 online).

Xenograft tumors induced by PDT-resistant SCC-13 cells

Trying to understand why some human tumors did not respond to PDT, we used the SCC-13 cells obtained from a moderately differentiated human SCC (Rheinwald and Beckett, 1981) and from the PDT-resistant populations (5thG and 10thG) (Supplementary Figure S3 online) to induce xenograft tumors in immunodeficient mice. When subcutaneous cells were injected into mice, the three cell types formed progressively growing tumors (Figure 2). Tumors induced by the 10^{th}G PDT-resistant cells were bigger than those induced by 5^{th}G PDT-resistant cells, which were in turn bigger than those caused by the parental cells ($P<0.01$) (Figure 2a). In addition, the number of tumors was significantly

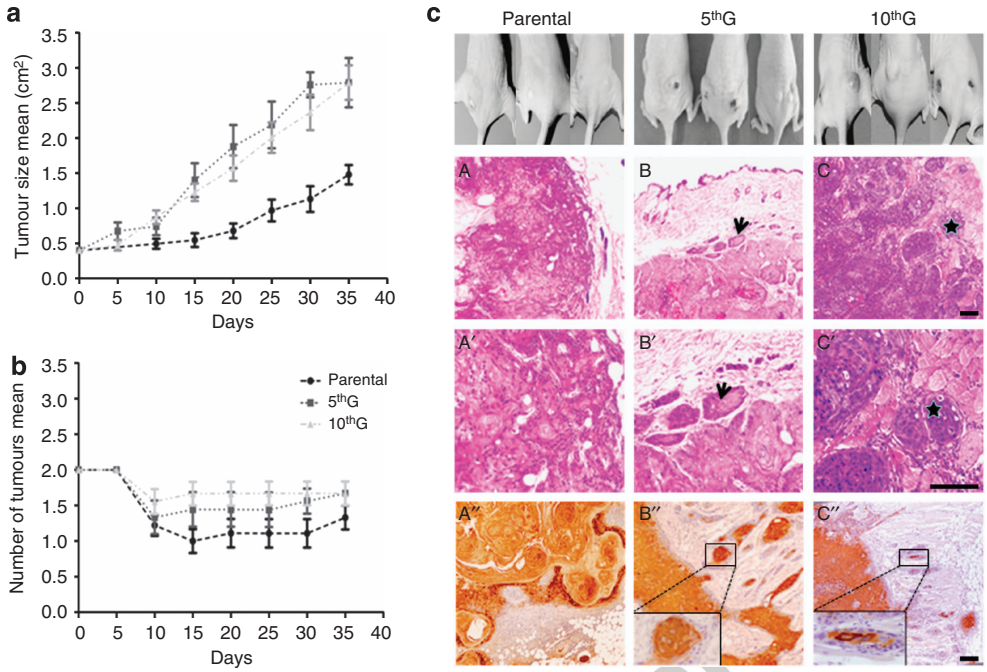

Figure 2. Xenograft tumors induced by parental, 5thG photodynamic therapy (PDT)-resistant, and 10thG PDT-resistant squamous cell carcinoma (SCC)-13 cells. (**a**) Growth curves of the tumors and (**b**) number of tumors per mouse. (**c**) Mice at the end of the experiment (upper panels) and histology (hematoxylin and eosin) of the tumors (medium and lower panels); (A) well-differentiated SCC with infiltrative masses of epithelial cells and horn pearls formation; (A′) detail showing infiltrative keratinocytes. (B) Moderately differentiated SCC with nests of atypical keratinocytes (arrow); (B′) micrometastases (arrow). (C) Poorly differentiated SCC with variable masses of atypical keratinocytes infiltrating skeletal muscle fibers (star); (Ć) detail from C, keratinocytes with nuclear pleomorphism (star); (A″–C″) Immunostaining against involucrin protein to highlight human cells forming the xenograft tumor: Inset in (C″) showing the low expression of involucrin. Scale bar = 200 μm.

higher in mice injected with resistant cells compared with those induced by parental cells; 8 of the total 14 injections with parental cells induced tumors, whereas with 5thG- and 10thG-resistant cells the number of injections required were 9 and 11, respectively. The differences between the mean number of tumors developed per mouse injected with the parental and resistant cells were statistically significant on days 15 and 30 ($P = 0.022$ and $P = 0.041$, respectively) (Figure 2b).

The histological characteristic of tumors induced by parental cells was the presence of mostly well (6/8)- or moderately (2/8) differentiated SCCs that tended to form one cyst per inoculation, encapsulated in a thin sphere of mouse dermal connective tissue (Figure 2cA and cA′). Similar results were obtained with some of the tumors induced by the 5thG PDT-resistant cells (Figure 2cB and cB′). Occasionally, parental and 5thG PDT-resistant cells induced tumors that grew invasively beyond the dermis (Figure 2cB and cB′). Conversely, despite the fact than three of the tumors induced by 10thG PDT-resistant cells were well differentiated, five of them were moderately or poorly differentiated SCCs, formed by atypical keratinocytes with nuclear pleomorphism even infiltrating skeletal muscle fibers (Figure 2bC and bC′). The immunostaining against involucrin (the antibody only reacts with the human protein) shows the lower expression of this protein in infiltrative cells of poorly differentiated tumors than in the well-differentiated ones (Said *et al.*, 1984; Lan *et al.*, 2013) (Figure 2cA″, cB″ and cC″).

Evaluation of aCGH of parental and PDT-resistant SCC-13 cell populations

As the development and progression of SCC is significantly correlated with the accumulation of genomic alterations, we next performed an array-based aCGH of the three cell types, parental, 5thG PDT-resistant, and 10thG PDT-resistant cells, to determine the potential genomic differences between them. The SCC-13 cell lines displayed multiple DNA copy-number alterations. Global results showing the genetic aberration profiles for all chromosomes are shown in Supplementary Figure S4 online; Supplementary Tables S1 and S2 online. Gains were more frequently observed than deletions. The significant gains were mostly mapped to several broad chromosomal regions including 1q, 3p, 5p, 7p, 8q, 11p, 12p, 17q, 19q, 20q, and chromosome X. Significant deletions were observed in 3p, 4q, 5q, 6q, 8p, 9p, 13q, and 21q. As a first approach, we focused our attention on specific well-known candidate genes of interest in cancer that mapped at determined amplified chromosomal regions. In this sense, all three cell types showed duplication in the cytobands: 7 p22.3p11.2 and 7p11.2 where the *EFGR* gene is located; amplification in 11q13.3q13.4 where *FGF3*, *FGF4*, and *CCND1* genes are situated; and trisomy in 17p13.1 where

Table 2. Some genomic amplifications in SCC-13 cells: parental, 5thG PDT-resistant, and 10thG PDT-resistant cells

Alteration	Chromosome	Cytoband location	Start	End	Size	Cell type	Genes of interest
Amplification	Chr5	5q11.2	56049292	56173104	0,123812	5G, 10G	*MAP3K1*
Duplication	Chr7	7p11.2	54412618	56267502	1,854884	P, 5G, 10G	*EGFR*
Duplication	Chr7	7p22.3p11.2	92332	57494582	57,40225	P, 5G, 10G	*EGFR*
Amplification	Chr11	11q13.3q13.4	68771683	71286976	2,515293	P, 5G, 10G	*FGF3, FGF4, CCND1*
Trisomy	Chr17	17p13.1	86809	80993148	80,906339	P, 5G, 10G	*TP53*

Abbreviations: PDT, photodynamic therapy; SCC, squamous cell carcinoma.

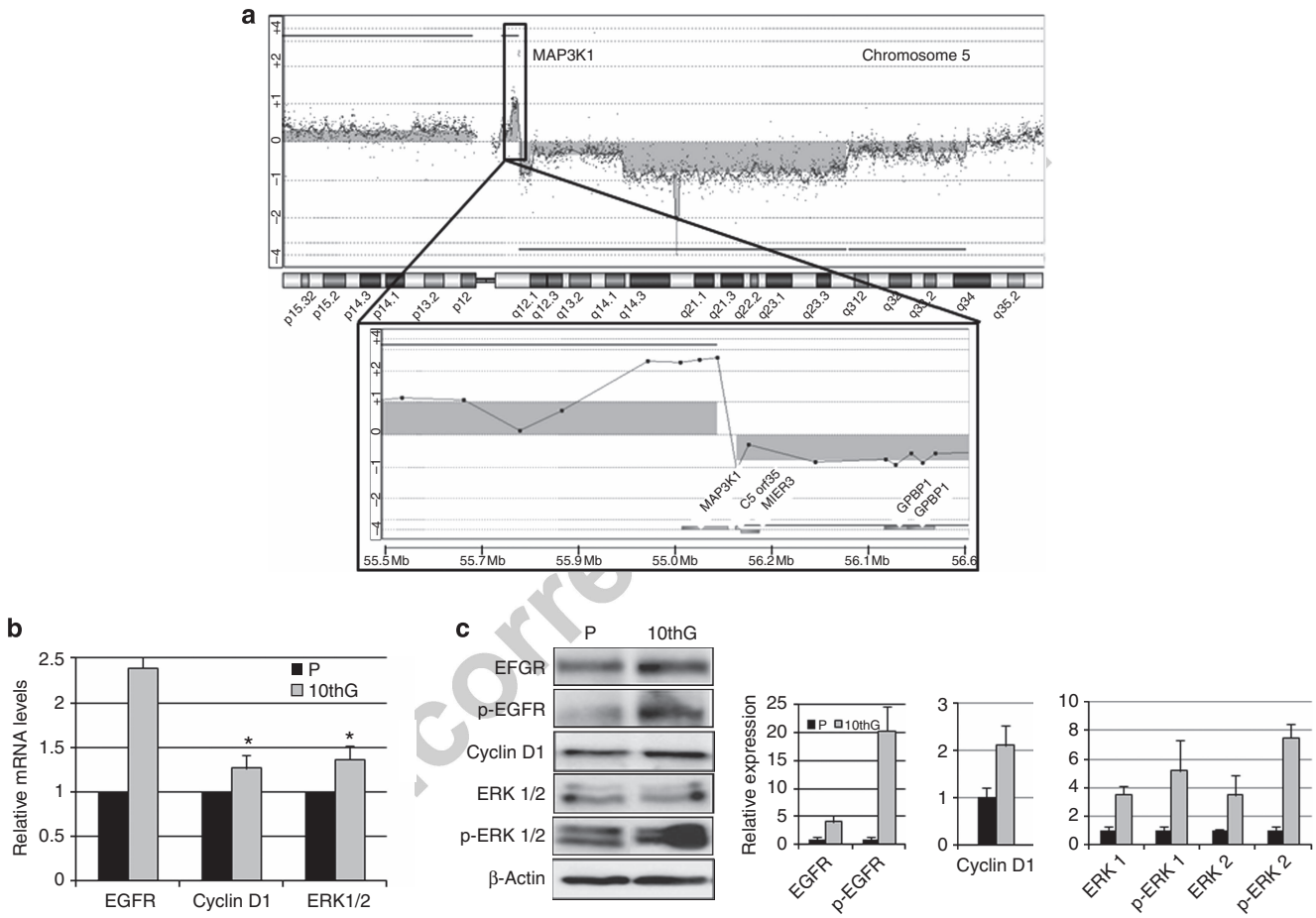

Figure 3. Molecular alterations detected in resistant SCC-13 cells. (**a**) Summary of copy-gain alterations of chromosomes 5 in 10thG-resistant SCC-13 cell population detected by aCGH according to the methodology used (array whole-human genome, AMADID 21924, statistical evaluation: ADM-2 A = 6 with at least five consecutive probes, ''moving average'' to 0.5 megabases). Enlargements of the 5q11.2 region identifies the gen codified for MAP3K1. (**b**) Levels of EGFR, cyclin D1, and ERK1/2 messenger RNAs (mRNAs) determined by real-time reverse-transcriptase PCR in SCC-13 cells (parental). The graph represents the fold values of the 10thG-resistant cells in relation to those of parental. (**c**) Western blot for different proteins (EGFR, cyclin D1, and ERK1/2) from extracts of parental and resistant photodynamic therapy cells (10thG) showing the increase in the expression of the evaluated proteins in resistant cells compared with that of parental; in the left panels, the densitometry of the corresponding bands are shown. *$P<0.05$.

TP53 is located (Table 2; Supplementary Figure S5 online). However, 5thG- and 10thG PDT-resistant cells presented, besides these, a distinctive amplicon in 5q11.2 corresponding to the *MAP3K1* gene among others (Table 2; Figure 3a). Main altered genes also located at the indicated cytobands are summarized in Supplementary Tables S1 and S2 online.

Potential implication of MAP3K1, EGFR, and cyclin D1 in the resistance of SCC to PDT

To validate the gains observed in chromosomes 5, 7, and 11 corresponding to the *MAP3K1*, *EGFR*, and *CCND1* loci and to interrogate the biological relevance of the functions of these genes, we next evaluated (i) the corresponding MAP3K1

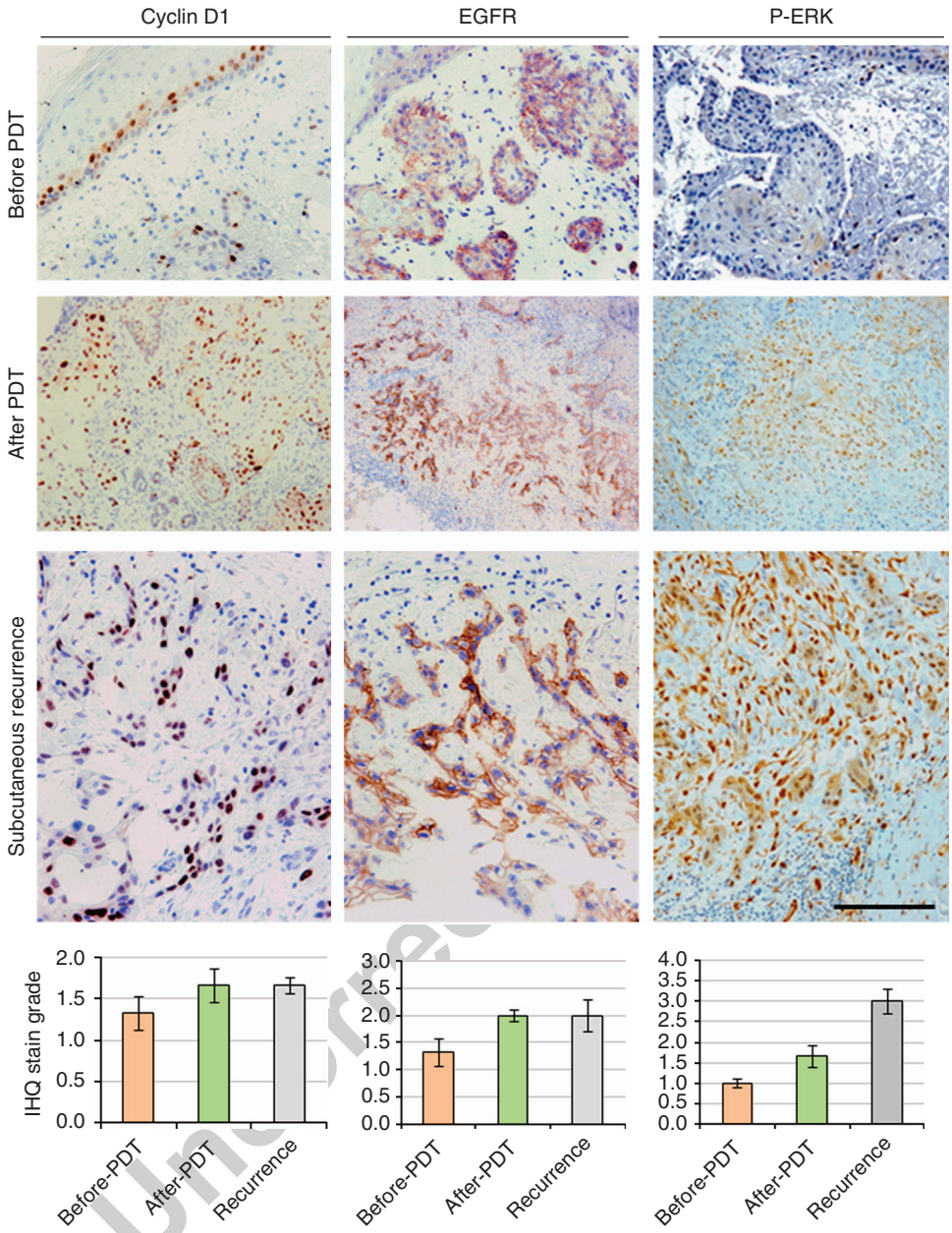

Figure 4. Immunohistochemical study of squamous cell carcinoma (SCC) with bad response to methyl-δ-aminolevulinic acid (MAL)-photodynamic therapy (PDT). First row shows a well-differentiated' SCC before MAL-PDT, second row a moderately differentiated infiltrating SCC after MAL-PDT, and third row the subcutaneous recurrence as a poorly differentiated SCC (case 2). Cyclin D1 immnunostaining in scattered tumor cells before MAL-PDT (A) being more intense and in a higher number of cells after PDT (A′, A″). EGFR immunodetection demonstrating a positive increasing expression before PDT (B) and (B′, B″) after three sessions of MAL-PDT (membranous staining). No signal of p-ERK was detected before PDT (C), but after PDT nuclear-positive staining was noted in the least-differentiated cells in the periphery of the tumor (C′), p-ERK was significantly increased with strong nuclear staining in the majority of tumor cells (C″). The graphs represent the results of immunohistochemical stains using a semiquantitative method translated into numbers to quantify them: 0 for negative, 1 for mild, 2 for moderate, and 3 for intense in the case of EGFR and cyclin D1, and from 0 to 4 for p-ERK. Scale bar = 200 μm.

(ERK1/2), EGFR, and cyclin D1 messenger RNA levels in SCC-13 cells by real-time reverse-transcriptase PCR and the expression of coded proteins by Western blot, and (ii) such coded proteins in the SCC biopsies obtained from the patients subjected to PDT by immunohistochemistry. Reverse-transcriptase PCR as well as western blot analysis of the SCC-13 cells (parental and 10^{th}G PDT-resistant cells) support the results obtained by aCGH; ERK1/2, EGFR, and cyclin D1 messenger RNAs appeared to be induced in 10^{th}G PDT-resistant cells and also the corresponding proteins showed strong expression, particularly EGFR and the phosphorylated active forms of ERK1/2 (Figure 3b and c).

The evaluation of the expression of MAP3K1 (ERK 1/2), EGFR, and cyclin D1 proteins as well as other markers related to the invasive capacity of cutaneous SCC including CD31, E-cadherin, and KI67 by immunohistochemistry in the patient biopsies is shown in Table 1; Figure 4. In the cases without response to PDT, we observed increased EGFR expression, except for case 1 who showed maximal expression already before the treatment (Supplementary Figure S6 online). A similar expression pattern was observed for cyclin D1, although to a lesser extent. KI67 and P53 did not show any consistency. In addition, the expression of p-ERK significantly increased after MAL-PDT in nonrespondent patients (Table 1); (Figure 4). Related to the cases with good response, the most remarkable finding was little or non-expression of EGFR and cyclin D1 in the tumors before the treatment (Table 1). All these results obtained either in the SCC-13 cultures or in patient biopsies indicate a role of *MAP3K1, EGFR,* and *CCND1* genes in the resistance to PDT.

DISCUSSION

MAL-PDT is one of the most effective treatments for NMSC. However, some relapses do occur. In this work, we have used patient samples and MAL-PDT-sensitive and MAL-PDT-resistant cells to analyze the genomic changes that may mediate the acquisition of refractoriness to MAL-PDT in SCC, and have focused on a handful of genes that crucially control tumor cell proliferation. SCC-13 cells resistant to MAL-PDT (5^{th} and 10^{th} PDT-resistant generations) (Milla *et al.*, 2011) presented a higher tumorigenic effect in immunodeficient mice than their parental cells and proved that genomic imbalances and overexpression of CCND1, EFGR, and MAP3K1 are involved in the development of clinical SCC resistance to PDT.

Only few studies have focused on recurrences and the aggressiveness of nonrespondent skin tumors to PDT. With respect to basal cell carcinoma, it has been described that post-PDT recurrences appear to display an increased histological aggressiveness (Fiechter *et al.*, 2012). Concerning SCC, the degree of cellular atypia has been proposed as a negative prognostic factor, suggesting that poorly differentiated keratinocytes are less susceptible to PDT (Calzavara-Pinton *et al.*, 2008). In our study, we have not found that the grade of differentiation of the SCC influenced the response to MAL-PDT. The only distinctive histological factor was the presence of an intense inflammatory lymphocytic infiltrate in the respondent tumors. Although this infiltrate is a prognostic factor in some tumors, such as melanoma, its significance in SCC is not clear (Azimi *et al.*, 2012). However, its presence could be considered as a host antitumoral response, which could contribute or even increase PDT effect (Talmadge, 2011).

Our data using aCGH clearly revealed the existence of chromosomal instability in SCC cells, both parental and those resistant to PDT. On applying aCGH, consistent amplification of the chromosomal region 11q13, which is associated with *CCND1,* has been detected in different stages of SCCs (Utikal *et al.*, 2005). Overexpression and genetic aberrations of EGFR have also been described in metastatic cutaneous SCCs (Shimizu *et al.*, 2001).

Cyclin D1 overexpression is frequently involved in keratinocyte carcinogenesis and it is an early event in cancer promotion (Alao, 2007; Jensen *et al.*, 2010). Our previous reports indicate that PDT reduces the expression of cyclin D1, KI67, and P53 in actinic keratosis (Bagazgoitia *et al.*, 2011). However, according to the present study, all the respondent patients were negative for cyclin D1, whereas the nonrespondents were positive and their expression increased after MAL-PDT. Therefore, cyclin D1 could be a differential marker between respondent and nonrespondent SCCs to MAL-PDT.

The EGFR pathway is very important in the therapeutic efficacy of PDT against cancer (Martinez-Carpio and Trelles, 2010). Array CGH revealed amplification of the chromosomal region 7p11.2, which leads to EGFR overexpression in primary and recurrent SCCs after MAL-PDT, although the reactivity patterns of such lesions were different. The primary tumors were weakly and focally positive, whereas the recurrences were diffusely and strongly positive. High expression of EGFR protein has been correlated with aggressiveness, poor prognosis, short survival, and development of resistance to cytotoxic agents in some tumors (Brabender *et al.*, 2001), including cutaneous SCCs (Shimizu *et al.*, 2001; Ch'ng *et al.*, 2008). Immunohistochemical analysis of our patients suggested that higher expression of EGFR before MAL-PDT could determine a bad response or may even increase the metastatic potential of the tumor. Furthermore, in cases of low expression, MAL-PDT could increase EGFR expression. Our results are consistent with those reported by Edmonds *et al.* (2012) who found that PDT stimulated EGFR phosphorylation and nuclear translocation, whereas the inhibition of EGFR signaling led to an increase of PDT cytotoxicity. Conversely, PDT has been shown to reduce the expression of EGFR in tumors induced by UVB in hairless mice (Ahmad *et al.*, 2001) and, within the time period of the reaction to PDT, normal and malignant cells lose their responsiveness to EGF and some cytokines (Martinez-Carpio and Trelles, 2010). The role of EGFR in the refractory response to PDT has been highlighted by the combination of PDT and EGFR inhibitors to act synergistically (Bhuvaneswari *et al.*, 2011; Postiglione *et al.*, 2013).

In addition, our results indicate that the mitogen-activated protein kinase MAP3K1 is increased in MAL-PDT-resistant 5^{th}G and 10^{th}G cells. The mitogen-activated protein kinase family drives cell proliferation, differentiation, and survival processes in different cell types. One of the mitogen-activated protein kinase-signaling cascades involved in most relevant human cancers is mediated by the phosphorylation of ERK1/2 (Roskoski, 2012). The elevated expression of p-ERK observed in SCCs in this study is consistent with high levels of the p-ERK frequently correlated with tumor aggressiveness and higher proliferative activity (Zhang *et al.*, 2007). In this sense, it has been described that sustained ERK1/2 activation protected cells from PDT (Tong *et al.*, 2002) and a recent study using A-431 epidermoid skin carcinoma and WiDr colorectal adenocarcinoma cells linked EGFR and ERK activation as a potential predictive factor for response to PDT (Weyergang *et al.*, 2013).

Our study raises the possibility that PDT favors the selection of more aggressive tumor cells and, taken together, these

results indicate that the MAPK/ERK signal pathway may be an important potential factor in the resistance to PDT. The activation of EGFR leads to sustained activation of ERK, activating the overexpression of cyclin D1, among other effects, and these signaling elements may counter the beneficial effect of PDT. Previous studies have demonstrated that MAL-PDT induces the production of reactive oxygen species, a key factor for the destruction of target cells; however, if some SCC cells received sublethal doses, it could promote a moderate production of endogenous reactive oxygen species, which efficiently stimulates cell growth, as it has been proven in human immortalized keratinocytes (HaCaT) (Blazquez-Castro *et al.*, 2012).

One of the limitations of our study is the size of the sample with only six patients. However, it has to be considered that MAL-PDT does not have an approved indication for invasive SCCs, therefore it is only exceptionally used. Another limitation is that we did not quantify the fluorescence of the PpIX accumulated in the tumor, therefore we cannot rule out that an insufficient conversion of MAL to PpIX could have contributed to the lack of response. However, this would not explain the change in tumor cells' aggressiveness.

In conclusion, our findings provide a better knowledge of the resistant mechanisms of SCCs to MAL-PDT and may contribute to well-informed patient selection when physicians are contemplating the use of PDT for SCCs. As aggressive cutaneous SCC can compromise the life of a patient, the results of our translational investigation support current clinical guidelines that recommend great caution when using PDT for invasive SCCs.

MATERIALS AND METHODS

Photosensitizers

For PDT in patients, a methyl derivative of MAL in cream (Metvix, Galderma, Spain) was used. For phototreatment of cell lines, MAL (Sigma-Aldrich, St Louis, MO) was prepared at a concentration of 10 mM in deionized sterile water. Appropriated dilutions were prepared in DMEM culture medium without serum.

Light sources

Patients were exposed to a monochromatic light source with a multi-light-emitting diode system (coherent light) 636 nm (Aktilite). For cell irradiation, a multi-light-emitting diode system (WP7143 SURC/E Kingsbright) of 635 ± 17 nm and an irradiation intensity of 6.2 mW cm^{-2} (as measured by Coherent Lasermate powermeter) was used.

Antibodies

The antibodies used were as follows: anti-rabbit polyclonal antibodies against ERK 1/2, p-ERK ½, AKT, p-AKT, FGF4, FGF8, cyclin D1, EGFR, KI67, anti-mouse monoclonal antibodies against E-cadherin, β-actin, Involucrin, P53, horseradish peroxidase mAb anti-IgG of mouse, and horseradish peroxidase mAb anti-IgG of rabbit (Supplementary Table S3 online).

RNA extraction and reverse-transcriptase PCR

Total RNA was extracted and purified with the RNAeasy Mini Kit (Qiagen). RNA from each sample was retrotranscribed to complementary DNA by the use of the "High capacity RNA to cDNA kit" (Applied Biosystems). Complementary DNA samples were used as templates for amplification reactions carried out with the LC480 SYBR Green I master (Roche Applied Science) following the manufacturer's instructions. Data from PCR amplifications were analyzed with LightCycler 480 software 1.5. Duplicate determinations were made, and the gene expression was determined by the ΔΔCt method using the probe Hs99999901_s1 18s rRNA as a reference gene. The primers used in this study were for human EGFR forward primer: 5′-TTTGCTGATTCAGGCTTGG-3′; reverse primer: 5′-AGAAAACTGACCATGTTGCTTG-3′ (Toby *et al.*, 2010) for human cyclin D1 forward: 5′-CCGTCCATGCGGAAGATC-3′; reverse 5′-GAAGACCTCCTCCTCGCACT-3′ (Medeiros *et al.*, 2002), for ERK1/2. forward: 5′-CCATTGGGTTGTGGAGGCAATG-3′, reverse: 5′-CACTCTGGGGATCAGTAAGGAC-3′ (Wang *et al.*, 2011).

Patients

Patients diagnosed with invasive cutaneous SCCs and treated with off-label MAL-PDT, because standard treatment options had been medically not recommended as first-line therapy, were included in the study. They were treated from January 2007 to December 2009 at the Dermatology Unit of Hospital San Jorge (Spain). Epidemiological, clinical, and histological data were collected (Table 1). Patients were subjected to PDT according to the approved procedure: curetting or debulking of the tumors, application of 160 mg g^{-1} MAL cream (Metvix) for 3 hours under occlusion and illumination with Aktilite (37 J cm^{-2}). PpIX fluorescence was routinely confirmed before irradiation and its disappearance after it.

Cell types

The cell line used was the SCC-13, obtained from a moderate SCC located on the face (Rheinwald and Beckett, 1981). Cells resistant to PDT were obtained as previously described (Milla *et al.*, 2011) by exposing the SCC-13 cells (parental) to several cycles of PDT (1 mM MAL, 4 hours of incubation and variable light doses of red light: 3.75, 5.5, 7.5, 11,5 J cm^{-2}). The final population received a total of 10 cycles of PDT (from 1st to the 10th resistant generation). Their resistance abilities were checked by the (3-[4,5-dimethylthiazol-2-yl]-2,5-diphenyltetrazoliumbromide) assay (Supplementary Figure S3 online). Cells were cultured under standard conditions in complete medium DMEM and antibiotics (Gibco Invitrogen, Carlsbad, CA).

Tumorigenicity assays of SCC-13 cells in nude mice

The *in vivo* tumorigenicity of cells was assessed in 2–3-month-old hairless athymic nude mice (AthymicNude-Foxn1nu, Harlan). The same number of cells in each case, parental, 5thG, and 10thG (10×10^6 cells in 0.3 ml of phosphate-buffered saline), was subcutaneously injected in each flank (right and left). The size of the tumors, blindly monitored weekly by the same investigator over 35 days, was calculated from calliper measurements of two ortogonal diameters. Seven mice were used for each SCC cell type. Mice were killed 35 days after administration of injections and tumors were fixed in neutral buffered formalin, sectioned in paraffin, and stained with hematoxylin and eosin or subjected to immunohistochemistry.

CGH array

For chromosomal aCGH, DNA of SCC-13 cells (parental, 5thG PDT-resistant and 10thG PDT-resistant generations) were isolated from exponential cultures using the Qiagen DNEasy Kit. Whole-genome

analysis of the cells was conducted using a commercial 60-k oligonucleotide human array-CGH (AMADID 21924, Agilent Technologies, Santa Clara, CA) following the manufacturer's protocol (Barrett *et al.*, 2004). Healthy female DNA (Promega Biotech, Madison, WI) was used as hybridization control. Microarray data were extracted and visualized using Feature Extraction software, v10.7 and Agilent Genomic Workbench, v5.0 (Agilent Technologies). Copy-number-altered regions were detected using ADM-2 (set as 6) statistic provided by DNA Analytics, with a minimum number of five consecutive probes. Microarray raw data tables have been deposited in the Gene Expression Omnibus under the accession number GSE50602

Western blots

For western blot, cells were lysed in radioimmunoprecipitation assay buffer (150 mM NaCl, 1% Triton X-100, 1% deoxycholate, 0.1% SDS, 10 mM Tris-HCl pH 7.2, 5mM EDTA, Phosphatase Cocktail, and Protease Inhibitor Cocktail) (Sigma-Aldrich). Protein concentrations were measured using the BCA Protein Assay Kit (Thermo Scientific Pierce, Rockford, IL). The proteins were electrophoresed, blotted on Immobilon-P PVDF membranes (Millipore, MA), and incubated with the first antibody overnight at 4 °C. Afterward, membranes were subjected to the peroxidase–conjugated secondary antibody and developed by chemiluminescence (ECL, Amersham Pharmacia Biotech, Little Chalfont, UK) using the high-definition system ChemiDoc XRS+ (Bio-Rad). The bands corresponding to the proteins were digitalized using the Image Lab, version 3.0.1 (Bio-Rad Laboratories), Adobe Photoshop 7.0 (Adobe Systems, USA), and Image J 1.44.

Immunohistochemistry

Sections of human and mice skin biopsies were subjected to automated immunostaining (TechMate 500, BioTech Solutions, Dako, Glostrup, Denmark) and then incubated in a detection kit (Chemate, code K4001, Dako) according to the manufacturer's instructions. Color was developed by 3-amino-9-ethylcarbazole solution as chromogen (Dako). Heat-induced epitope retrieval was performed using a pressure cooker. Representative sections were examined using positive and negative controls. The antibodies used are in the Supplementary Table S1 online. Evaluation of immunohistochemical staining was performed by counting the number of cells with a grid that expressed the antigen studied, in 10 high-magnification representative fields. The percentage of positive cells was established for P53 and KI67, whereas a semiquantitative method was used for EGFR and cyclin D1 ($0 \leqslant 10\%$ of the tumor cells staining; mild = light (intensity) and incomplete (quality) staining in $>10\%$; moderate = moderate and complete staining of $>10\%$; and intense = intense and complete staining $>10\%$) (Sweeny *et al.*, 2012) and p-ERK: grade 1: $<5\%$; grade 2: 5–25%; grade 3: 26–50%; and grade 4: $>50\%$ of positive cells (Zhang *et al.*, 2007). To represent the results graphically, the semiquantitave staining measures were translated into numbers: 0 for negative, 1 for mild, 2 for moderate, and 3 for intense in the case of EGFR and cyclin D1, and from 0 to 4 for p-ERK. To avoid interobserver variability, the same pathologist evaluated all samples and he was blind for the clinical data of the patients.

Microscopy and statistical treatments

Microscopic observations were made with a microscope Olympus BX61 with a CCD digital camera DP50 and processed using the Adobe PhotoShop CS5 Extended, version 12.0 (Adobe Systems).

The values in the figures and tables are expressed as mean and SE. Comparisons among the means of the number and size of induced tumors in mice as well as among the means of the (3-[4,5-dimethylthiazol-2-yl]-2,5-diphenyltetrazoliumbromide) assay were made using analysis of variance test for those variables with normal distribution and the Kruskal–Wallis tests for those deviating from them. The threshold for statistical significance was set at $P<0.05$. Analysis was performed using the STATA software (STATA, Version 7.0, StataCorp, College Station, TX).

Ethics

Treatment procedures in patients and the study of their skin samples were approved by the Ethics Committee for Clinical Investigation of Aragón, Spain (protocol number PI12/0096) and signed consent was obtained. All clinical investigations were conducted according to the Declaration of Helsinki Principles. Mice were used in accordance with the guidelines approved by institutional Animal care and Ethics Committee from Universidad Autónoma of Madrid.

CONFLICT OF INTEREST

The authors state no conflict of interest.

ACKNOWLEDGMENTS

The work was supported by MINECO (FIS PI12/01253), and Comunidad de Madrid (S2010/BMD-2359). We recognize the valuable contributions of Javier Suela and Juan Cruz Cigudosa.

SUPPLEMENTARY MATERIAL

Supplementary material is linked to the online version of the paper at http://www.nature.com/jid

REFERENCES

Agostinis P, Berg K, Cengel KA *et al.* (2011) Photodynamic therapy of cancer: an update. *CA Cancer J Clin* 61:250–81

Ahmad N, Kalka K, Mukhtar H (2001) In vitro and in vivo inhibition of epidermal growth factor receptor-tyrosine kinase pathway by photodynamic therapy. *Oncogene* 20:2314–7

Alao JP (2007) The regulation of cyclin D1 degradation: roles in cancer development and the potential for therapeutic invention. *Mol Cancer* 6:24

Azimi F, Scolyer RA, Rumcheva P *et al.* (2012) Tumor-infiltrating lymphocyte grade is an independent predictor of sentinel lymph node status and survival in patients with cutaneous melanoma. *J Clin Oncol* 30:2678–83

Bagazgoitia L, Cuevas Santos J, Juarranz A *et al.* (2011) Photodynamic therapy reduces the histological features of actinic damage and the expression of early oncogenic markers. *Br J Dermatol* 165:144–51

Barrett MT, Scheffer A, Ben-Dor A *et al.* (2004) Comparative genomic hybridization using oligonucleotide microarrays and total genomic DNA. *Proc Natl Acad Sci USA* 101:17765–70

Bhuvaneswari R, Yuen GY, Chee SK *et al.* (2011) Antiangiogenesis agents avastin and erbitux enhance the efficacy of photodynamic therapy in a murine bladder tumor model. *Lasers Surg Med* 43:651–62

Blazquez-Castro A, Carrasco E, Calvo MI *et al.* (2012) Protoporphyrin IX-dependent photodynamic production of endogenous ROS stimulates cell proliferation. *Eur J Cell Biol* 91:216–23

Brabender J, Danenberg KD, Metzger R *et al.* (2001) Epidermal growth factor receptor and HER2-neu mRNA expression in non-small cell lung cancer Is correlated with survival. *Clin Cancer Res* 7:1850–5

Calzavara-Pinton PG, Venturini M, Sala R *et al.* (2008) Methylaminolaevulinate-based photodynamic therapy of Bowen's disease and squamous cell carcinoma. *Br J Dermatol* 159:137–44

Ch'ng S, Low I, Ng D *et al.* (2008) Epidermal growth factor receptor: a novel biomarker for aggressive head and neck cutaneous squamous cell carcinoma. *Hum Pathol* 39:344–9

Edmonds C, Hagan S, Gallagher-Colombo SM *et al.* (2012) Photodynamic therapy activated signaling from epidermal growth factor receptor and STAT3: targeting survival pathways to increase PDT efficacy in ovarian and lung cancer. *Cancer Biol Ther* 13:1463–70

Fai D, Arpaia N, Romano I *et al.* (2009) Methyl-aminolevulinate photodynamic therapy for the treatment of actinic keratoses and non-melanoma skin cancers: a retrospective analysis of response in 462 patients. *G Ital Dermatol Venereol* 144:281–5

Fiechter S, Skaria A, Nievergelt H *et al.* (2012) Facial basal cell carcinomas recurring after photodynamic therapy: a retrospective analysis of histological subtypes. *Dermatology* 224:346–51

Jensen V, Prasad AR, Smith A *et al.* (2010) Prognostic criteria for squamous cell cancer of the skin. *J Surg Res* 159:509–16

Juarranz A, Jaen P, Sanz-Rodriguez F *et al.* (2008) Photodynamic therapy of cancer. Basic principles and applications. *Clin Transl Oncol* 10:148–54

Lan YJ, Chen H, Chen JQ *et al.* (2013) Immunolocalization of vimentin, keratin 17, Ki-67, involucrin, beta-catenin and E-cadherin in cutaneous squamous cell carcinoma. *Pathol Oncol Res*

Q22

Lomas A, Leonardi-Bee J, Bath-Hextall F (2012) A systematic review of worldwide incidence of nonmelanoma skin cancer. *Br J Dermatol* 166:1069–80

Martinez-Carpio PA, Trelles MA (2010) The role of epidermal growth factor receptor in photodynamic therapy: a review of the literature and proposal for future investigation. *Lasers Med Sci* 25:767–71

Medeiros LJ, Hai S, Thomazy VA *et al.* (2002) Real-time RT-PCR assay for quantifying cyclin D1 mRNA in B-cell non-Hodgkin's lymphomas. *Mod Pathol* 15:556–64

Milla LN, Cogno IS, Rodriguez ME *et al.* (2011) Isolation and characterization of squamous carcinoma cells resistant to photodynamic therapy. *J Cell Biochem* 112:2266–78

Morton CA, McKenna KE, Rhodes LE British Association of Dermatologists Therapy Guidelines, Audit Subcommittee, the British Photodermatology Group (2008) Guidelines for topical photodynamic therapy: update. *Br J Dermatol* 159:1245–66

Neville JA, Welch E, Leffell DJ (2007) Management of nonmelanoma skin cancer in 2007. *Nat Clin Pract Oncol* 4:462–9

Ortiz-Policarpio B, Lui H (2009) Methyl aminolevulinate-PDT for actinic keratoses and superficial nonmelanoma skin cancers. *Skin Therapy Lett* 14:1–3

Postiglione I, Chiaviello A, Aloj SM *et al.* (2013) 5-aminolaevulinic acid/photodynamic therapy and gefitinib in non-small cell lung cancer cell lines: a potential strategy to improve gefitinib therapeutic efficacy. *Cell Prolif* 46:382–95

Rheinwald JG, Beckett MA (1981) Tumorigenic keratinocyte lines requiring anchorage and fibroblast support cultured from human squamous cell carcinomas. *Cancer Res* 41:1657–63

Roskoski R Jr. (2012) ERK1/2 MAP kinases: structure, function, and regulation. *Pharmacol Res* 66:105–43

Said JW, Sassoon AF, Shintaku IP *et al.* (1984) Involucrin in squamous and basal cell carcinomas of the skin: an immunohistochemical study. *J Invest Dermatol* 82:449–52

Shimizu T, Izumi H, Oga A *et al.* (2001) Epidermal growth factor receptor overexpression and genetic aberrations in metastatic squamous-cell carcinoma of the skin. *Dermatology* 202:203–6

Stebbins WG, Hanke CW (2011) MAL-PDT for difficult to treat nonmelanoma skin cancer. *Dermatol Ther* 24:82–93

Sweeny L, Dean NR, Magnuson JS *et al.* (2012) EGFR expression in advanced head and neck cutaneous squamous cell carcinoma. *Head Neck* 34: 681–6

Talmadge JE (2011) Immune cell infiltration of primary and metastatic lesions: mechanisms and clinical impact. *Semin Cancer Biol* 21:131–8

Toby IT, Chicoine LG, Cui H *et al.* (2010) Hypoxia-induced proliferation of human pulmonary microvascular endothelial cells depends on epidermal growth factor receptor tyrosine kinase activation. *Am J Physiol Lung Cell Mol Physiol* 298:L600–6

Tong Z, Singh G, Rainbow AJ (2002) Sustained activation of the extracellular signal-regulated kinase pathway protects cells from photofrin-mediated photodynamic therapy. *Cancer Res* 62:5528–35

Utikal J, Udart M, Leiter U *et al.* (2005) Numerical abnormalities of the Cyclin D1 gene locus on chromosome 11q13 in non-melanoma skin cancer. *Cancer Lett* 219:197–204

Wang K, Zhang M, Qian YY *et al.* (2011) Imbalanced expression of mitogen-activated protein kinase phosphatase-1 and phosphorylated extracellular signal-regulated kinases in lung squamous cell carcinoma. *J Zhejiang Univ Sci B* 12:828–34

Weyergang A, Selbo PK, Berg K (2013) Sustained ERK [corrected] inhibition by EGFR targeting therapies is a predictive factor for synergistic cytotoxicity with PDT as neoadjuvant therapy. *Biochim Biophys Acta* 1830:2659–70

Zhang X, Makino T, Muchemwa FC *et al.* (2007) Activation of the extracellular signal-regulated kinases signaling pathway in squamous cell carcinoma of the skin. *Biosci Trends* 1:156–60